

Direct current magnetic insulation of an immersed RF antenna

M A Jaworski, B E Jurczyk, Erik L Antonsen and D N Ruzic

Plasma-Material Interaction Group, University of Illinois at Urbana-Champaign, Urbana, IL 61801 USA

E-mail: mjaworsk@uiuc.edu

Received 24 August 2005, in final form 26 April 2006

Published 23 May 2006

Online at stacks.iop.org/PSST/15/474

Abstract

A weak DC magnetic field is applied to an immersed helical resonator antenna in an RF plasma to study the effects of magnetic insulation on potential differences between plasma and antenna within the vacuum chamber. Past research suggests a link between minimizing antenna potential and mitigating self-sputtering effects within the chamber to minimize debris creation. Alteration of particle flux ratios at the sheath boundary affects this potential difference. A simplified theory of cross-field diffusion shows the trend of decreasing potential as a function of the Hall parameter. A Langmuir probe obtains experimental evidence showing a continuously decreasing potential at lower Hall parameters than theory predicts. Due to RF biasing of the plasma, alteration of the diffusion coefficient is not the only variable affecting the potential difference between plasma and antenna. Since the experiments focus on the transitional state between collisional and magnetized plasmas, inclusion of collisional physics in the next iteration of theory may predict trends in the potential difference between plasma and antenna potential more accurately. The normalized potential difference between plasma and antenna is shown to decrease by 35% over a ten-fold increase in the Hall parameter where simplified theory predicts no change.

1. Introduction

The semiconductor industry is moving to shorter wavelengths of light to continue the miniaturization of integrated circuits. Extreme ultraviolet (EUV) light at 13.5 nm is the next wavelength expected for lithography by chip manufacturers. One of the challenges to producing a high volume manufacturing tool with these advanced light sources is the high amount of debris produced along with the light that can damage collector optics present in the chamber.

The Illinois debris mitigation experimental applications laboratory (IDEAL) is a test-bed for debris mitigation studies. One method currently under investigation is the use of a secondary RF plasma. An internal antenna must be used to generate the RF plasma because of metal coating and contamination concerns when operating with a dielectric window. Several studies of internal antennae immersed in the plasma have been carried out [1–3]. An immediate issue found with work with immersed antennae is that of antenna biasing of

the plasma. This biasing of the plasma leads to self-sputtering of the antenna and high plasma potentials that may interfere with processing.

Various means of reducing the plasma potential have been investigated in the past. These include the application of a DC current on the antenna [1]. This DC current produces a magnetic field next to the antenna and has been shown to greatly reduce the potential difference between the plasma and the antenna. A floating antenna configuration [3] was shown to be effective in also reducing the floating potential of the plasma itself. The use of electrostatic shields or Faraday shields [4] has also been employed. These electrostatic shields have been shown to reduce capacitive coupling between the antenna and the plasma. They have also been shown to reduce the coupling efficiency to the plasma [2]. Finally, so-called balanced inductive sources or helical resonators [5, 6] have been designed such that antenna lengths become long with respect to the electrical wavelength. In these devices, the electrical potential of the RF wave balances negative with

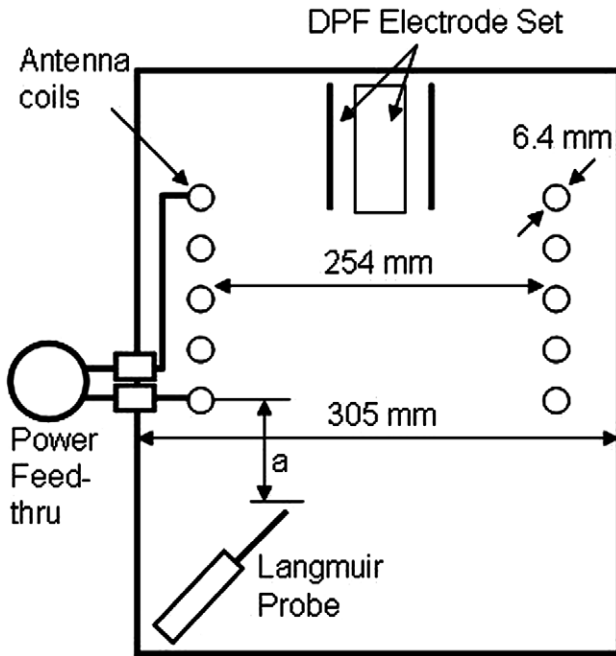


Figure 1. Diagram of the IDEAL chamber and location of major components of the experiment.

positive over the length of the antenna as a whole. The net effect is that the antenna as a whole remains neutral.

Of present interest is the use of magnetic fields to reduce the plasma floating potential. Theoretical considerations of a surface in a magnetized plasma have been considered [7–9] in addition to experimental studies [10]. In all these cases the magnetic fields are such that the electron gyro radius is much smaller than the debye length of the plasma. These field strengths and conditions are applicable mostly to fusion science studies but are not often found in cold processing plasmas.

This work is undertaken to present data taken on the IDEAL experiment. The IDEAL system uses a number of methods for reducing the plasma potential described above. The magnetic fields produced in these experiments are much lower than those treated in a previous work on magnetized sheaths [7–10]. A reduction in potential difference between the plasma and the antenna is observed and some simplified physics are suggested to explain these observations.

2. Apparatus and approach

A stainless steel chamber 30.5 cm in diameter and 42.5 cm in height is used for these experiments. Additional debris mitigation experiments use a dense plasma focus (DPF) electrode set at the top of the chamber. A near half wavelength helical resonator antenna with a diameter of 25.4 cm with 5 turns over 12.7 cm is wound in the chamber. This antenna is supplied with RF power and cooling water through isolated Conflat feed-throughs. A schematic of the chamber and antenna is presented in figure 1.

RF power is supplied to the device in a number of stages. A type B+K Precision E-2000 variable oscillator drives an ENI A-500 class A solid-state RF amplifier. This amplifier

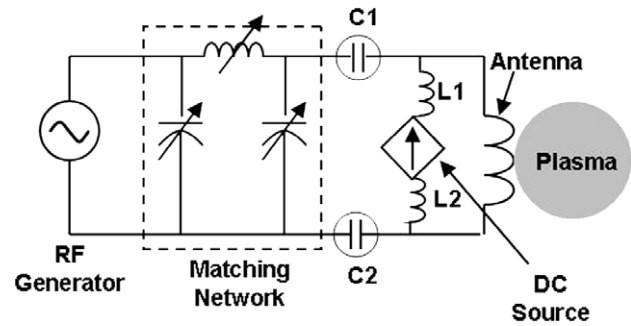


Figure 2. Electrical diagram of an RF power system and a DC power system. Capacitors C1 and C2 allow the antenna and DC source to float. Inductors L1 and L2 prevent the RF power from reaching the DC source.

feeds a vacuum tube driven power amplifier (PlasmaTherm type HFS 500E). The output from the vacuum tube amplifier feeds the antenna through a custom made pi-type matching network. The antenna is isolated from the chamber by the CF power feed-thrus and from the RF network by two blocking capacitors.

In addition to the ability to supply RF power to the system, an EMS 7.5–130 high current DC supply is used. The supply connects through a large inductor on the positive and negative sides of the antenna. The circuit system can be seen in figure 2.

Measurements of plasma density and temperature are taken with an RF compensated Langmuir probe [11]. The probe sits in a fixed position approximately 9 cm in from the wall and 4 cm below the antenna itself. During the operation of the RF plasma, the voltage on the probe tip is swept positive and negative in order to build a Langmuir probe trace. This allows determination of the plasma density and temperature. The RF compensation of the probe is tuned to block 28 MHz signals and the second harmonic at 56 MHz.

The data presented here are taken in a continuous series of points. The two major inputs to the system which are varied are RF power and DC current to the antenna. For a given constant DC current to the antenna, the incident power is varied from 10 to 200 W. Both incident and reflected power are monitored. For this paper, the incident power is maintained at the reported value and the reflected power is minimized by rematching the system as necessary. Seven different DC current values are taken from 0 to 120 A. In all, this yields 28 total data points.

Pressure in the chamber is monitored with a MKS type 627 pressure transducer pressure gauge. For all of these tests, argon is the background gas with a fill pressure of 10 mtorr. The incident and reflected power are read from the tube amplifier. The antenna potential is measured with a Fluke 177 True RMS multimeter. The multimeter attaches to the positive terminal of the DC current source and measures the antenna potential through a large inductor.

3. Theory

By passing a DC current through the antenna, a magnetic field is formed around the antenna itself. A weaker solenoidal field is produced by the entire antenna structure; however, this field is smaller than that found locally around the conductor itself. As a result of the strong local field, electrons which would

normally escape the plasma to the antenna are trapped in the magnetic field surrounding it or are reflected by the sheath electric field. In addition to reducing the potential of the plasma itself, this may also prevent a floating antenna from charging to a low potential.

In sheath theory, the floating potential of a surface exposed to a plasma results from the mass and energy imbalance between electrons and ions in the plasma. Electrons move far faster than ions and an electric potential arises between the surface and the bulk plasma. Equation (1) describes the relationship as discussed in Chodura [8]

$$\frac{e\phi_w}{T_e} \approx \ln\left(\frac{\Gamma_i}{\Gamma_e}\right), \quad (1)$$

where ϕ_w is the wall potential with respect to the plasma potential at zero, T_e is the electron temperature and $\Gamma_{i,e}$ is the incoming flux of ions or electrons, respectively. In typical processing plasmas assuming cold ions, the flux of ions at the sheath/pre-sheath boundary is assumed to follow the Bohm sheath criterion. Using the Bohm sheath criterion, the ratio of the fluxes becomes dependent only on the mass of the ionic species present in the plasma [12]. The wall potential is then given as

$$\frac{e\phi_w}{T_e} = \left(3.34 + \frac{1}{2} \ln \mu\right), \quad (2)$$

where μ is the atomic mass number. In order to alter the wall potential, one can then examine what terms are included in the flux of each species. Equation (3) gives the flux of a charged species in a plasma [13]

$$\Gamma_s = \pm \mu_s n E - D_s \nabla n, \quad (3)$$

where μ_s is the species mobility, n is the density, E is the electric field vector, D_s is the species diffusion coefficient and ∇n is the gradient of the density. In the case of diffusion across a magnetic field both the diffusion coefficient and the mobility change are given in equations (4) and (5) as follows.

$$\mu_{\perp} = \frac{\mu_s}{1 + (\omega_c \tau_m)^2}, \quad (4)$$

$$D_{\perp} = \frac{D_s}{1 + (\omega_c \tau_m)^2}, \quad (5)$$

where ω_c is the cyclotron frequency for the species and τ_m is the mean time to a collision event. In the case of low fields, as are present in these experiments, the ion mobility and diffusion constants remain unaltered. The same cannot be said for electron mobility and diffusivity. For the sake of simplicity it is assumed that the ion flux remains constant over low fields. Changes in the electric field and density gradient are likewise neglected as they are beyond the scope of the present paper. Equation (6) then is the expected behaviour of the wall potential with the application of a magnetic field:

$$\frac{e\phi_w}{T_e} \approx \ln\left[\frac{\Gamma_{i0}}{\Gamma_{e0}} (1 + (\omega_c \tau_m)^2)\right]. \quad (6)$$

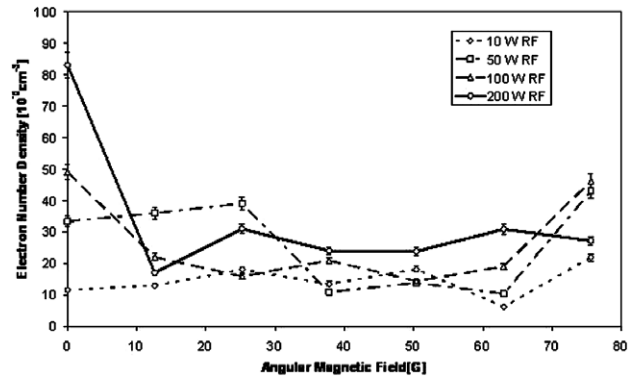


Figure 3. Electron number density versus applied magnetic field for four different input powers. The decrease in density with applied field is due to the plasma confinement away from the Langmuir probe location. Field strength is calculated at the surface of the antenna conductor. The probe is situated away from the antenna center to prevent arcing.

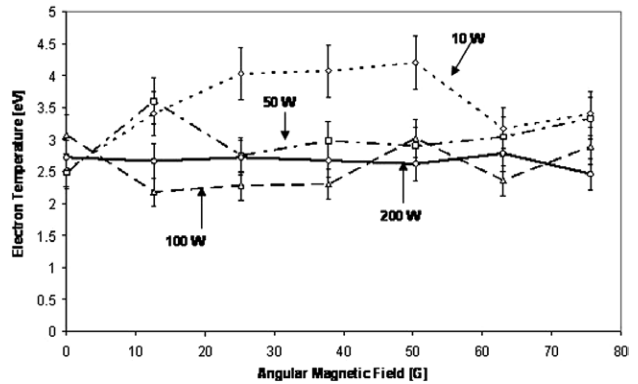


Figure 4. Electron temperature versus the angular magnetic field for four different input powers. Field strength is calculated at the surface of the antenna conductor.

4. Experimental results

With the application of higher powers and magnetic fields, little effect was measured on the number density of the plasma, nor the electron temperature. Figures 3 and 4 show plots of these quantities as a function of the antenna magnetic field parametrized by incident RF power. Visual inspection of the plasma with increasing magnetic field revealed that the plasma brightness increased within the confines of the antenna but that density throughout the chamber was not affected significantly. The data shown in figure 3 exhibits an initial drop in density with applied field for all but the 10 W input power case. This drop in density is due to the Langmuir probe being located outside the solenoid of the helical resonator antenna. The lack of a density decrease in the 10 W case is possibly due to the high amount of capacitive coupling between the antenna and the chamber at low power levels. At higher power levels, there is more inductive coupling inside the antenna helix than outside the antenna coil where the probe is located. In the 50 W data, there is a drop in density between 25 and 38 G as opposed to between 0 and 12 G in 100 and 200 W. This delayed density drop could be indicative of a change in coupling mode from capacitive to inductive. The higher electron temperatures at low power shown in figure 4 may be due to a higher fraction of

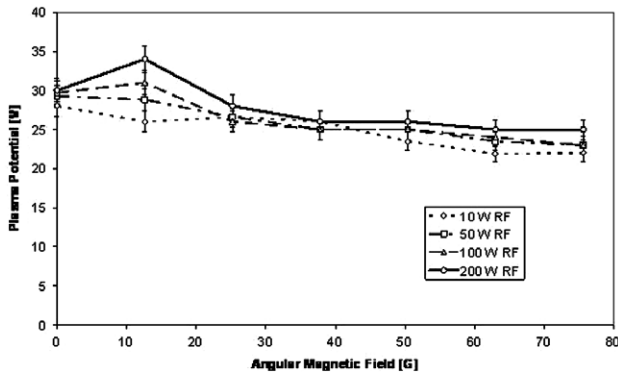


Figure 5. Plasma potential versus the angular magnetic field for four different input powers. The angular magnetic field is calculated at the surface of the conductor.

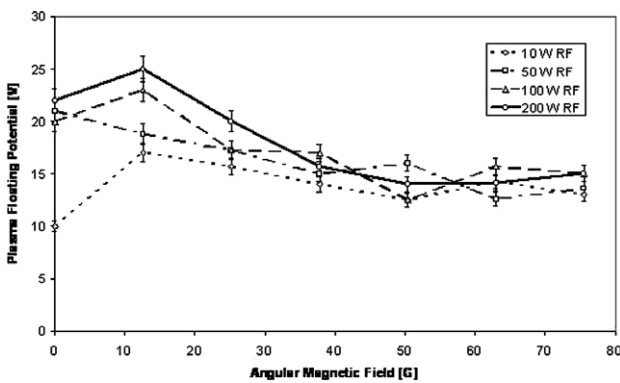


Figure 6. Plasma floating potential versus angular magnetic field for four different input powers. Field strength is calculated at the surface of the antenna conductor.

capacitive coupling driving electron motion where the probe is located. As soon as the DC current is increased the plasma pulls in towards the antenna region.

Plasma potential and floating potential are more global quantities and the probe's location is adequate to measure changes in these quantities. The plasma potential is obtained by determining the maximum of the absolute value of the first derivative of the Langmuir $I-V$ curve. In applying the DC field it was observed that the plasma conditions, such as matching conditions and plasma luminosity, changed almost immediately. It is hypothesized that this is due to gross changes to the effective geometry of the plasma device with the imposed DC field. As such, the trends indicating an increase in potentials at about 10 G could have occurred much sooner and the lines provided in the figures are only to guide the eyes. After this initial increase the measured plasma potential and floating potential both decrease with increasing applied magnetic field. Figures 5 and 6 show the results of the analysis. Note that if the probe is located higher in the chamber, arcing often occurs to the probe tip invalidating the probe results.

Figure 7 shows the difference between the plasma potential and the antenna potential. The antenna potential is measured by the multimeter attached at inductor L2. The magnitude of the potential drop between the antenna and the plasma is as high as 260 V. The antenna potential goes far negative with increasing power. The applied magnetic field affects this antenna potential more than the plasma potential;

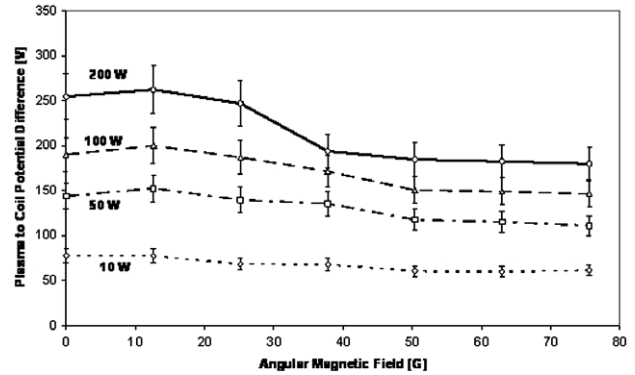


Figure 7. Plasma to antenna potential difference versus angular magnetic field for four different input powers. Field strength is calculated at the surface of the antenna conductor.

however, both contribute to the decrease in the difference between the two. The difference between the two is also observed to decrease at higher power.

5. Discussion

A floating antenna configuration allows the antenna to self-bias negative as opposed to biasing the plasma positive. Antenna self-biasing increases with input power. The source of this effect is unclear but it is thought that several possible mechanisms may contribute to it. The first is an increase in the flux imbalance between electrons and ions arriving at the antenna which may also explain the lack of large density increases observed with increasing power as shown in figure 3. Another mechanism may be the acceleration of electrons by RF potentials increasing the antenna potential to plasma potential difference. Additional electrons that are produced in the system, instead of contributing to the density of the plasma, may be contributing to the bias of the antenna and driving it further negative.

This phenomenon also suggests that at the power levels at which the device is operating, the plasma is capacitively coupled to the antenna. Due to the floating antenna configuration, though, instead of driving the plasma potential higher, the antenna is driven further negative while the plasma potential remains fairly constant with incident power. This capacitive coupling results in a biasing of the normalized plasma potential.

The application of a magnetic field shows an effect upon reducing this self-biasing of the antenna. At 200 W, the potential drop between the plasma and the antenna decreases by 30% with the application of 75 G at the antenna surface. While the potential drop remains constant beyond the 38 G data point, the normalized wall-plasma potential, discussed below, continues decreasing with increasing field as shown in figure 8. This decrease is not as significant as those found in other experiments [1]; however, the difference between the applied fields is significant.

Figure 8 shows the normalized wall-plasma potential difference, N , versus the Hall parameter, $\omega_c \tau_m$, for the data taken with the IDEAL experiment and data published by Nakamura *et al* [1] for similar conditions. The value of the magnetic field is taken at the debye sheath boundary. In this

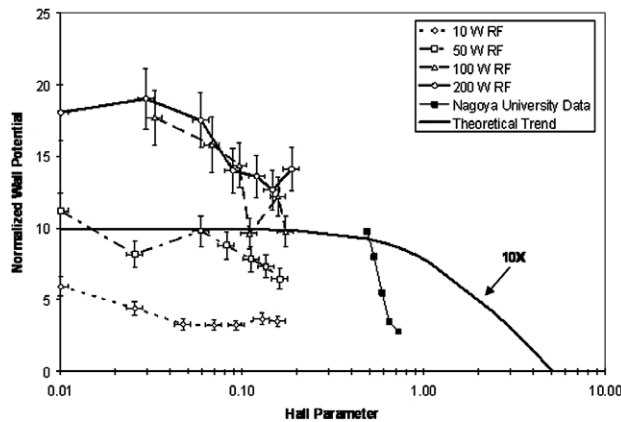


Figure 8. Normalized wall potential N versus Hall parameter $\omega_c \tau_m$ for four input power levels and 200 W, 10 mTorr Nagoya University data [1]. The theoretical data trend is shown at 10X for comparison purposes. A Hall parameter value of unity indicates a full electron cyclotron revolution before a collision event occurs.

figure, the normalized wall-plasma potential is defined as in equation (7) as follows.

$$N = \frac{V_p - V_{\text{coil}}}{T_e (3.34 + \ln \mu)} \quad (7)$$

where N is the normalized wall-plasma potential difference, V_p is the measured plasma potential, V_{coil} is the measured antenna potential, T_e is the electron temperature in electron volts and μ is the ion mass. In the case of the data from Nagoya University, the antenna potential was taken to be ground due to the experimental set-up reported and the measured plasma potential was used. The normalized wall-plasma potential is the ratio of the measured plasma–antenna potential difference to the floating potential difference expected based on electron temperature and ion mass. This number is a non-dimensional indicator of the potential between a biased object in the plasma to that of a floating object in the plasma. If the theoretical potential difference is present between the antenna and the plasma, then the value of N would be unity. The theoretical trend presented in the graph is that given by equation (6).

Instantly noticeable in this figure is the large biasing measured in the experiments. This is believed to be an effect of RF sheath biasing briefly mentioned above and in [1,3] and a result of capacitive coupling to the plasma. While there does seem to be some scatter in the data there is a general trend in reducing the normalized wall potential whereas the theoretical trend is fairly flat until a hall value of 0.5 when it begins to dip negative. The average reduction in N for all input powers is 35%. The data trends may be indicative of non-linear effects on the electric field in the pre-sheath and changes in the density gradient caused by the rise of a magnetic pre-sheath.

According to Chodura [8], the size of the magnetic presheath affects the potential distribution near a plasma boundary. In non-magnetized plasmas, the debye sheath is on the order of ≈ 4 debye lengths. In a magnetized plasma, the presheath may cause the potential drop in the sheath and pre-sheath to be spread to 20 debye lengths or more. This alteration in the electric field would affect the density profile and drift terms governing the sheath calculations. The trend in the data indicates that these additional effects may be important

in altering the ratio of electron and ion fluxes reaching the antenna. These may also include collisional effects in the magnetic and debye pre-sheaths as well as the second order effects mentioned above.

6. Conclusions

A novel immersed antenna plasma configuration has been tested in the IDEAL chamber. A floating helical resonator antenna has been demonstrated as a means of producing a secondary plasma for further studies of debris mitigation. Over the range of input powers, the antenna is driven negative with respect to the chamber ground with increasing power. Due to the created potential drop between the plasma and antenna, the floating antenna configuration does not reduce self-sputtering of the antenna by itself. However, by maintaining a smaller plasma potential with respect to ground, sputtering of chamber walls can be minimized.

Application of a DC current is shown to be effective at reducing the potential drop between the plasma and the antenna in this configuration. However, RF biasing still plays a significant role in the determination of the plasma potential. The data indicates that alteration of the diffusion coefficient due to the magnetic field is not the only term affecting the potential drop between the plasma and the powered antenna.

Acknowledgments

The authors wish to express their thanks to a great many people who have made this research possible. The first is Robert Bristol and Intel Corporation for providing funding for this project under SRA #159-03. For providing invaluable technical assistance on the project as a consultant: Mike Williams. Finally, a group of dedicated undergraduates working in the PMI Group too numerous to name individually deserve thanks as well. Their hard work and dedication made this research possible.

References

- [1] Nakamura K, Kuwashita Y and Sugai H 1995 *Japan. J. Appl. Phys.* **34** L1686
- [2] Suzuki K, Nakamura K, Ohkubo H and Sugai H 1998 *Plasma Sources Sci. Technol.* **7** 13
- [3] Setsuhara Y, Miyake S, Sakawa Y and Shoji T 1999 *Japan. J. Appl. Phys.* **38** 4263
- [4] Sugai H, Nakamura K and Suzuki K 1994 *Japan. J. Appl. Phys.* **33** 2189
- [5] Vinogradov G K and Yoneyama S 1996 *Japan. J. Appl. Phys.* **35** L1130
- [6] Vinogradov G K, Menagarishvili V M and Yoneyama S 1998 *J. Vac. Sci. Technol. A* **16** 3164
- [7] Daybelge U and Bein B 1981 *Phys. Fluids* **24** 1190
- [8] Chodura R 1982 *Phys. Fluids* **25** 1628
- [9] Riemann K-U 1994 *Phys. Plasmas* **1** 552
- [10] Koch B, Bohmeyer W and Fussmann G 2003 *J. Nucl. Mater.* **313–316** 1114
- [11] Sudit I and Chen F F 1994 *Plasma Sources Sci. Technol.* **3** 162
- [12] Ruzic D N 1994 *Electric Probes for Low Temperature Plasmas* (New York: American Vacuum Society)
- [13] Lieberman M A and Lichtenberg A J 1994 *Principles of Plasma Discharges and Materials Processing* (New York: Wiley)